

DOI: 10.24425/118955

A. MAURYA\*, P. KUMAR JHA\*\*

## STUDY OF FLUID FLOW AND SOLIDIFICATION IN BILLET CASTER CONTINUOUS CASTING MOLD WITH ELECTROMAGNETIC STIRRING

Electromagnetic stirrer generates swirling fluid flow, boosts the mixing of molten steel near the solidification front and enhances the quality of the continuously cast products. In the present investigation, attention is paid towards studying the effect of in-mold electromagnetic stirring on fluid flow and solidification. A three-dimensional coupled mathematical model of solidification and magnetohydrodynamics has been established for billet caster mold. The alternating magnetic field is applied to the solidification model where fluid flow, heat transfer, and electromagnetic equations are solved simultaneously. It has been found that an increase in field frequency decreases the length of stirring and the liquid fraction of the steel at the center of the mold exit. Tangential velocity near the solidification front increases with the magnetic field frequency or flux density, due to which, a break in solidified shell near stirrer position is predicted whose width increases accordingly.

*Keywords:* Continuous casting, mold, electromagnetic stirring, fluid flow, solidification

### List of symbols

$\vec{B}$	– Magnetic flux density
$\vec{D}$	– Electric flux density
$\vec{E}$	– Electric field strength
$\vec{H}$	– Magnetic field strength
$\vec{j}$	– Electric current density
$q$	– Electric charge density
$\vec{U}$	– Fluid velocity
$\epsilon$	– Electric permittivity
$\sigma$	– Electrical conductivity
$\mu$	– Magnetic permeability
$\vec{F}$	– Lorentz force
$\vec{B}_0$	– External magnetic flux density
$\vec{b}$	– Induced magnetic flux density
$h_w$	– Heat transfer coefficient
$c_p$	– Specific heat
$q_w$	– Wall heat flux
$T_w$	– Wall temperature
$T_a$	– Ambient temperature
$H_o$	– Enthalpy of steel
$\rho$	– Density of steel
$k_{eff}$	– Effective conductivity
$Q_L$	– Source term
$L$	– Latent heat
$\beta$	– Liquid fraction
$\vec{U}_{pull}$	– Pull velocity

$T_{solidus}$	– Solidus temperature
$T_{liquidus}$	– Liquidus temperature
$\mu_{eff}$	– Effective viscosity
$\vec{g}$	– Acceleration due to gravity
$S$	– Momentum sink term
$A_{mush}$	– Mushy zone constant
$k$	– Turbulent kinetic energy
$\epsilon$	– Dissipation rate

### 1. Introduction

During solidification in the continuous casting mold, dendritic grains grow towards the mold center and liquid metal get trapped in the primary inter-dendritic arm spacing. These regions typically characterize a mushy zone where both liquid and solid phases co-exist. The principle use of in-mold electromagnetic stirring (M-EMS) is to continuously stir the liquid zone and the mushy zone within the mold. Stirring about mold axis moves the high-temperature molten metal towards the mushy zone and attempts to transform mush to liquid by re-melting the solidified grains. This liquid flow usually breaks the dendrites formed at the solid front and induces grain manipulation [1].

Over the last few decades, intense attention has been paid on M-EMS continuous casting steel industries due to its metallurgical usefulness in controlling the quality of steel [2,3]. Controlled stirring of molten steel within the mold effectively reduces inclu-

\* DEPARTMENT OF MECHANICAL AND INDUSTRIAL ENGINEERING, INDIAN INSTITUTE OF TECHNOLOGY ROORKEE, UTTARAKHAND-247667, INDIA

\*\* Corresponding author: pkjhafme@iitr.ac.in

sions, minimizes the central shrinkage porosity and centerline segregation and enhances the proportion of equiaxed grains and fine dendritic structure [1]. M-EMS is reported to improve the homogeneity [4] in initial solidification and suppresses oscillation marks [5]. It rapidly reduces the degree of superheat of the molten metal which promotes equiaxed grain formation [6]. It has been reported that current intensity and frequency of the stirrer have a significant impact on the columnar and equiaxed grain structure [7] of the metal cast. Toh et al. [8] predicted that using low-frequency electromagnetic field at mold top, increase in magnetic field density resulted into decrease in surface roughness and depth of oscillation marks on cast metal surface. Sahoo et al. [9] found a significant increase in the length of the equiaxed zone and reduction in central shrinkage and central cracks with increase in EMS current up to 280 A, going beyond which mold powder entrapment at the surface of billet and increase in erosion of submerged entry nozzle was found. Using macro/micro model, Govindaraju and Li [10] have shown the pronounced effect of EMS on the nucleation and grain growth by microstructure analysis. Wang et al. [11] have reported 10% increase in central equiaxed crystal ratio by the use of M-EMS at 300 A current intensity, the Wang et al. [12] further predicted 30% increase in the central equiaxed zone with 310 A EMS current intensity in 40CrMo4 steel grade billet.

Several mathematical models [8,13] have been developed by researchers related to the application of EMS, investigating the flow behavior of molten metal in the mold (M-EMS), secondary solidification (S-EMS), and final solidification (F-EMS) zone. Liu et al. [14] numerically predicted that increase in stirring current and decrease in frequency increases the magnitude of magnetic flux generated by electromagnetic stirrer while the stirring current was reported to be linearly proportional to tangential velocity [15] of fluid flow.

In-appropriate use of EMS has produced adverse effects like formation of white band and loss of resources. Thus, it is important to use stirrer of requisite capacity to induce optimum stirring effects. It is better to understand the metal flow behavior and its consequences on the solidification behaviour and related metallurgical effects on the cast metal. Numerical simulation is an effective way to study the electromagnetic stirring technology as it reduces the cost of resources on experiments, material and manpower. A large number of previously reported literature were focused towards the generation of electromagnetic field and its effect on the fluid flow by varying the process parameter of magnetic field generation. Many researchers [16] studied the effect of EMS using finite element method (FEM) and fluid flow using either FEM or by coupling it with finite volume method. In reality, a solution using FEM needs large computational resource requirement and simulation time as well. Several researcher [4,17,18] have advocated to use simplified coupling method where, a constant and homogeneous magnetic flux density having rotary nature is being used instead of stray magnetic field. The suggested magnetic field commendably forecast the role of EMS in the continuous casting mold.

In the present work, numerical investigation of fluid flow in the mold with the application of electromagnetic stirrer and

its effect on solidification by applying heat transfer conditions in the model has been carried out. Electromagnetic field equations have been discretised and solved simultaneously with fluid flow, heat transfer and solidification equations using finite volume method. A constant and homogeneous magnetic flux density having rotary nature has been considered. The parameters such as magnitude of magnetic flux density and frequency have been varied to investigate its effect on solidification characteristics inside the mold.

## 2. Mathematical formulation

During the continuous casting of steel, electromagnetic stirrer generates an alternating magnetic field that passes through the molten steel. As molten steel is a conductor of electricity, an eddy current is induced in it, which generates electromagnetic force called Lorentz force. The generated Lorentz force is rotary in nature and guide the fluid to rotate accordingly. In the present study, the Maxwell's equations are solved to find the electromagnetic forces through applied magnetic field. These forces are added to the momentum conservation equations in Navier-Stokes equation as a source term. The three-dimensional coupled model of fluid flow, heat transfer, solidification and electromagnetic field is solved and analysed to study the solidification behaviour inside the mold.

### 2.1. Electromagnetic equations

The basic concept behind the EMS model is coupling between the fluid flow and Lorentz force generated due to the interaction of induced eddy current and applied magnetic field. The Maxwell's equations describing the electromagnetic field are given as:

$$\nabla \cdot \vec{B} = 0 \quad (1)$$

$$\nabla \times \vec{E} = -\frac{\partial \vec{B}}{\partial t} \quad (2)$$

$$\nabla \cdot \vec{D} = q \quad (3)$$

$$\nabla \times \vec{H} = \vec{j} + \frac{\partial \vec{D}}{\partial t} \quad (4)$$

where,  $\vec{H}$  and  $\vec{E}$  are magnetic and electric field intensities respectively.  $\vec{B}$  and  $\vec{D}$  are flux densities for magnetic and electric field respectively.  $q$  is electric charge density while  $\vec{j}$  is electric current density vector.  $\vec{H}$  and  $\vec{D}$  can be written in the following form:

$$\vec{H} = \frac{1}{\mu} \vec{B} \quad (5)$$

$$\vec{D} = \epsilon \vec{E} \quad (6)$$

where,  $\mu$  and  $\epsilon$  are magnetic permeability and electric permittivity of the liquid metal.

Ohm's law was defined for current density in the media having electrical conductivity  $\sigma$  as:

$$\vec{j} = \sigma \vec{E} \quad (7)$$

In a magnetic field  $\vec{B}$  and fluid velocity field  $\vec{U}$ , Ohm's law is redefined as:

$$\vec{j} = \sigma (\vec{E} + \vec{U} \times \vec{B}) \quad (8)$$

Now, the induction equation derived from the above Ohm's law and Maxwell's equation is in the form:

$$\frac{\partial \vec{B}}{\partial t} + (\vec{U} \cdot \nabla) \vec{B} = \frac{1}{\mu \sigma} \nabla^2 \vec{B} + (\vec{B} \cdot \nabla) \vec{U} \quad (9)$$

The total magnetic field  $\vec{B}$  in the fluid will be  $\vec{B}_0 + \vec{b}$ . Since in the present study, magnetic field  $\vec{B}_0$  is imposed externally which is independent of flow velocity while, induced magnetic field  $\vec{b}$  is caused by the impact of flow velocity and is required to be solved. Thus, Eq. (9) can be simplified for external magnetic field as:

$$\frac{\partial \vec{B}_0}{\partial t} = \frac{1}{\mu \sigma} \nabla^2 \vec{B}_0 \quad (10)$$

The induced magnetic field [19] can be calculated inserting Eq. (10) in Eq. (9):

$$\begin{aligned} \frac{\partial \vec{b}}{\partial t} + (\vec{U} \cdot \nabla) \vec{b} &= \frac{1}{\mu \sigma} \nabla^2 \vec{b} + \\ &+ \left[ (\vec{B}_0 + \vec{b}) \cdot \nabla \right] \vec{U} - (\vec{U} \cdot \nabla) \vec{B}_0 \end{aligned} \quad (11)$$

The Lorentz force is generated by the total magnetic field in the fluid which is further added in the momentum equation – Eq. (19),

$$\vec{F} = \vec{j} \times \vec{B} = \vec{j} \times (\vec{B}_0 + \vec{b}) \quad (12)$$

## 2.2. Solidification equations

Energy conservation equation for solidification is defined as

$$\rho \frac{\partial H}{\partial t} + \rho \nabla \cdot (\vec{U} H_o) = \nabla \cdot (k_{eff} \nabla T) + Q_L \quad (13)$$

where,  $Q_L$  is source term and  $H_o$  is the total enthalpy of the material which can be computed as the sum of sensible heat ( $h$ ) and latent heat content ( $\Delta H_o$ ),  $k_{eff}$  is effective conductivity.

Sensible enthalpy and latent heat content at reference temperature " $T_{ref}$ " with reference enthalpy " $h_{ref}$ " and latent heat of material " $L$ " are defined as,

$$h = h_{ref} + \int_{T_{ref}}^T c_p dT \quad (14)$$

$$\Delta H_o = L \beta \quad (15)$$

where,  $\beta$  is liquid fraction at temperature " $T$ ".

The source term  $Q_L$  has two terms in it: explicit latent heat term which describes the liquid/solid transformation and convective term which consider the pulling of solidified shell at a constant casting velocity " $\vec{U}_{pull}$ ". In a single phase solidification model,  $Q_L$  can be expressed as:

$$Q_L = \rho L \frac{\partial (1 - \beta)}{\partial t} + \rho L \vec{U}_{pull} \cdot \nabla (1 - \beta) \quad (16)$$

In Eq. (16), latent heat (L) has been used because the source term is associated with the phase change and describes the rate of latent heat evolution during the phase change or liquid/solid transformation. The region having solid fraction value of one will move along the casting direction with the casting speed. It is to be noted that the term  $(1 - \beta)$  shows the solid fraction of the material. The liquid fraction can be calculated by determining the temperature [20,21] as:

$$\beta = \begin{cases} 0 & \text{if } T < T_{solidus} \\ \frac{T - T_{solidus}}{T_{liquidus} - T_{solidus}} & \text{if } T_{solidus} < T < T_{liquidus} \\ 1 & \text{if } T > T_{liquidus} \end{cases} \quad (17)$$

## 2.3. Fluid flow equations

The continuity equation and transient momentum conservation Navier-Stokes equation can be expressed respectively as:

$$\nabla \cdot \vec{U} = 0 \quad (18)$$

$$\begin{aligned} \frac{\partial}{\partial t} (\rho \vec{U}) + \rho \nabla \cdot (\vec{U} \vec{U}) &= -\nabla P + \\ &+ \nabla \cdot \left\{ \mu_{eff} (\nabla \cdot \vec{U}) \right\} + \rho \vec{g} + S + \vec{F} \end{aligned} \quad (19)$$

Effective viscosity " $\mu_{eff}$ " is the sum of dynamic viscosity " $\mu_l$ " and turbulent viscosity " $\mu_t$ ". For solidification, enthalpy-porosity technique is being used where the mushy zone is treated as pseudo porous medium and the porosity of each cell will be the liquid fraction in that cell. The porosity of porous medium indicates the liquid content in solid or liquid dispersed in solid dendrites. When the porosity of the cell equals to zero, the cell will be treated as completely solidified and velocity in that zone extinguishes as there is no liquid. To move the solidified zone in the casting direction, the momentum sink term " $S$ " is added to the right-hand side of the Navier-Stokes equation (Eq. 19). This moves the newly solidified material at a constant pull velocity which is set equals to the casting velocity. The momentum sink term [20] can be expressed as:

$$S = \frac{(1 - \beta)^2}{(\beta^3 + \xi)} A_{mush} (\vec{U} - \vec{U}_{pull}) \quad (20)$$

A very small positive constant  $\xi$  is provided in the denominator of Eq. (20) to avoid zero in the denominator.  $A_{mush}$  is a mushy zone constant and is influenced by the grain morphol-

ogy [22] at the solidification front. So, care must be taken while assigning a value to it. In the present model, the value of mushy zone constant is taken as  $10^6$ . In the momentum sink term, the relative velocity between the molten liquid and the solid is used rather than the absolute velocity of the liquid.

Turbulence in the mold has been calculated using realizable  $k$ - $\varepsilon$  turbulence model as it avoids the singularity at a low value of turbulence [23,24], which are found in the mushy zone. Shih et al. [25] have reported the realizable  $k$ - $\varepsilon$  turbulence model as most suitable for solidification model. The two partial differential equations for turbulent kinetic energy ( $k$ ) and dissipation rate ( $\varepsilon$ ) are given by

$$\rho \frac{\partial k}{\partial t} + \nabla \cdot (\rho k \bar{U}) = \nabla \cdot [(\mu_t + \alpha_k \mu_t) \nabla k] + G - \rho \varepsilon + S_k \quad (21)$$

$$\rho \frac{\partial \varepsilon}{\partial t} + \nabla \cdot (\rho \varepsilon \bar{U}) = \nabla \cdot [(\mu_t + \alpha_\varepsilon \mu_t) \nabla \varepsilon] + C_{1\varepsilon} \frac{\varepsilon}{k} G - C_{2\varepsilon} \rho \frac{\varepsilon^2}{k + \sqrt{\nu \varepsilon}} + S_\varepsilon \quad (22)$$

where, respectively.  $\alpha_k$  and  $\alpha_\varepsilon$  are the inverse effective Prandtl numbers,  $C_{1\varepsilon} = 1.44$  and  $C_{2\varepsilon}^* = 1.92$  [26,27] are the model parameters,  $G$  is the generation of the turbulence kinetic energy due to mean velocity gradients.

In Eq. (22), it can be seen that denominator of realizable  $k$ - $\varepsilon$  model never vanishes even if  $k$  is zero, which is not the case with the standard  $k$ - $\varepsilon$  model. Sinks  $S_k$  and  $S_\varepsilon$  are added to the turbulence kinetic and dissipation equations respectively, in the mushy and solidified zones to account for the presence of solid matter.

## 2.4. Computational details

Figure 1(a) shows the 3-dimensional geometrical model of the billet caster mold, along with its physical dimensions. The diameter of the mold inlet is 46 mm. At the inlet and outlet of the mold, velocity of the steel entering and leaving the mold respectively are constant and their values are calculated by balancing mass flow rate in the mold at casting speed of 1.8 m/min. The steel entering the mold is also kept at constant temperature with 8 K of superheat over liquidus temperature. It is assumed that heat transfer from the meniscus is negligible as compared to the mold wall. For heat ejection from the mold wall a constant heat transfer coefficient ( $h_w = 1.2 \text{ MW/m}^2\text{K}$ ) is provided [28]. The mold wall heat flux ( $q_w$ ) can be expressed as:

$$q_w = h_w A (T_w - T_a) \quad (23)$$

$T_w$  and  $T_a = 300 \text{ K}$  are the mold wall temperature and ambient temperature respectively [29]. At the mold wall, viscous no slip boundary condition is being used and solidified shell formed due to the application of solidification model near the mold walls is set to move with casting speed. During electromagnetic field

calculation, to avoid the passing of induced electric current from the mold wall, a perfect electrically insulating wall is being used. The model was divided into 111335 cells while the concern has been made at the vicinity of the wall with the fine grid (Fig. 1b) as EMS and solidification both has significant consequences [30] over that region. Figure 1(b) also shows the average shell thickness at the mold wall for the case without EMS. The alternating magnetic field with constant homogenous magnetic flux density is applied at the stirrer region of 100 mm wide, placed 350 mm below the meniscus as shown in Figure 1(a).

All the governing equations were discretized and solved using finite volume method based CFD tool Ansys Fluent. The second order implicit scheme was used to provide a higher order of accuracy. The magnetic field in  $x$ - $y$  direction has been applied using the Fluent Magnetohydrodynamic (MHD) addon module. The solution was executed in a transient state with an initial time step of 0.0001 seconds and further after getting convergence, it is gradually increased to 0.01 seconds. The solution convergence has been achieved with momentum residuals  $<10^{-4}$  and energy residuals  $<10^{-7}$ . Computation time of each simulation was approximately 20 days on a workstation of 8GB RAM and six-core AMD Opteron(tm) processor.

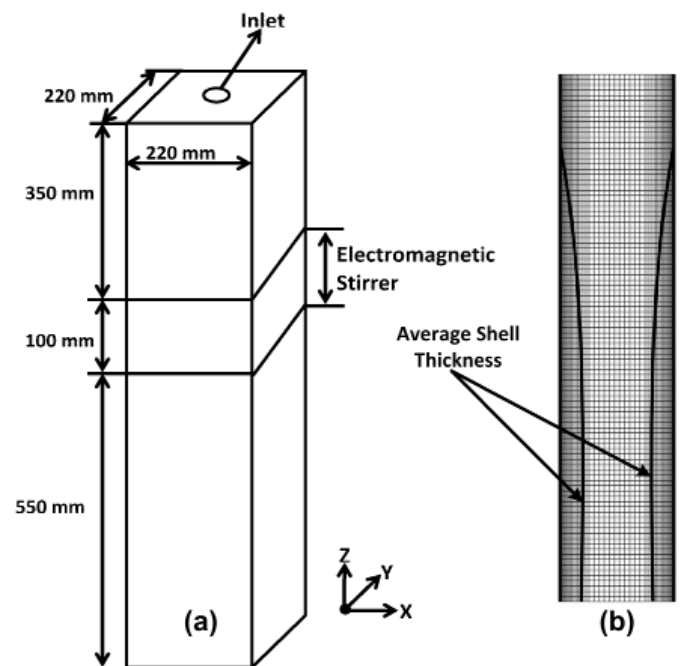


Fig. 1. (a) Model Geometry of billet caster mold (b) Computational grid at mold wall

In order to simplify the model, assumptions were made while solving governing equations. Liquid steel was considered as Newtonian incompressible fluid while its density, specific heat, and magnetic permeability are considered invariant. Mold oscillation, effect of segregation, shrinkage due to solidification, etc. has been ignored. Joule heating due to the induced eddy currents has been ignored. For electromagnetic equations, the boundary condition for induced magnetic field is assumed to be tangential to the wall, so that induced fields are closed inside the

mold and do not cross the boundary. Other boundary conditions and material properties used are listed in Table 1.

TABLE 1

Boundary conditions and material properties [31] used in present work

Boundary conditions/Material properties	Value
Casting speed (m/min)	1.8
Inlet temperature (K)	1813
Liquidus temperature (K)	1805
Solidus temperature (K)	1792
Density of molten steel (Kg/m <sup>3</sup> )	7200
Viscosity of molten steel (Kg/ms)	0.0067
Specific heat (J/KgK)	750
Thermal conductivity (W/mK)	41
Latent heat (J/Kg)	272000
Electrical conductivity (1/Ωm)	$7.14 \times 10^5$
Magnetic permeability (H/m)	$1.257 \times 10^{-6}$

### 3. Model validation

To ensure the correctness of the results obtained using numerical investigation, both solidification and electromagnetic field MHD models have been validated separately. For validation of both the models, separate geometries have been prepared according to details reported in the previous works of Nakato et al. [32] and Im et al. [18] for solidification and EMS, respectively. Nakato et al. have experimentally measured the solid shell thickness profile on the center of narrow wall of a slab caster mold along the casting direction. The shell thickness at the narrow wall predicted by the present solidification model is shown in Figure 2(a), which closely matches with the shell thickness measured by Nakato et al. A three-dimensional numerical investigation of the square billet by placing the stirrer of 0.4 m width in the middle of the computational domain of length 1.6 m has been performed by Im et al. They have predicted the turbulence kinetic energy in the z-direction and advocated that turbulent kinetic energy efficiently measures the stirring efficiency and

strength of shear at the solid wall. The EMS model has been discretely validated by calculating the turbulence kinetic energy at two different positions on the reported model and boundary conditions by Im et al. It can be seen in Figure 2(b) that both the reported and present predicted curves of turbulent kinetic energy closely matches with each other, which defines the trust worthiness of the present EMS model.

### 4. Results and discussion

Three-dimensional fluid flow analysis with coupled solidification and EMS in a billet caster mold has been carried out. Effect of electromagnetic stirring on solidification has been studied by varying the frequency of magnetic field and magnetic flux density. The computational model was also analyzed by individually applying solidification and EMS model in the mold. Figure 3(a) shows the velocity vector at a lateral plane in the middle of stirrer position, where the velocity vectors can be seen in the form of dots when only solidification model has been applied. This is due to fluid flow predominantly in the z-direction and nearly negligible velocity components in x and y-direction. On the other hand, after applying only EMS model with magnetic flux density and frequency of 0.1 T and 10 Hz respectively, the effect of electromagnetic stirring in the form of rotary motion of the fluid in x-y direction can be seen in Figure 3(b). The fluid has high velocity in x and y-direction at the outer side and gradually decreases toward the center. This high-velocity flow near the solidification front is expected to break down the coarse columnar dendritic solidification structure to produce a finer structure. However, in Figure 3(c) the predicted vector distribution of Lorentz force at a lateral plane in the middle of stirrer has been shown. It can be seen that the Lorentz forces are maximum at one diagonal corner and minimum along the other diagonal. These diagonal forces will set a rotary motion in the liquid steel. Further, on finding the Lorentz force distribution at a different time step, it is found that though the direction of Lorentz forces changes with time because of the alternating behavior of the magnetic field, the direction of rotation remains the same. The

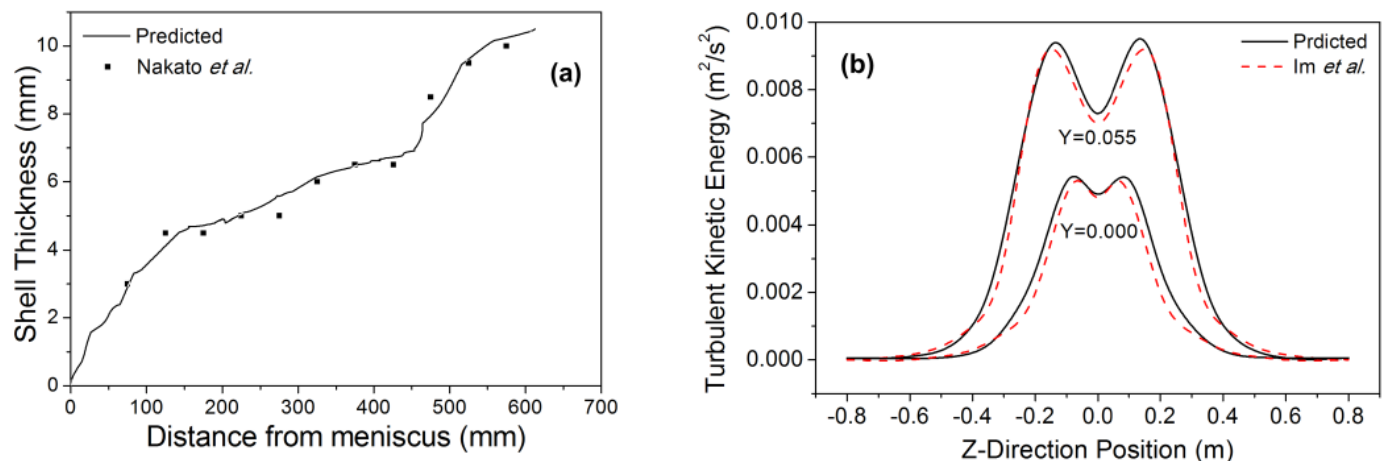


Fig. 2. Validation of (a) Solidification model (b) EMS model

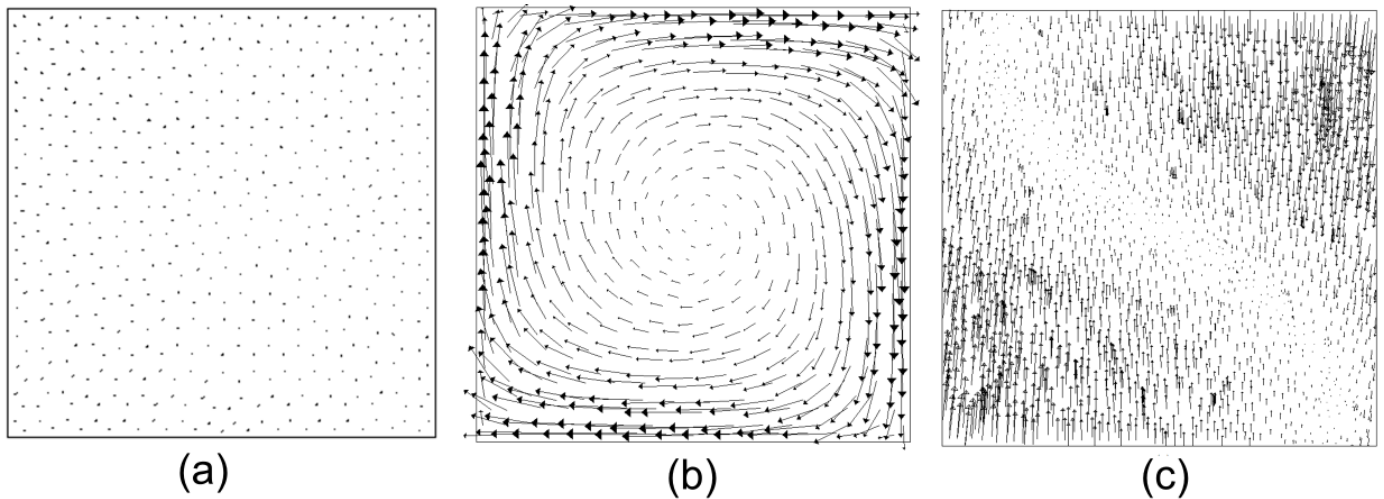


Fig. 3. Velocity vector for fluid flow (a) with solidification (b) with electromagnetic field, and (c) Vector distribution of Lorentz force under electromagnetic field

position of maximum forces moves along the periphery of the mold while at the center, the magnitude is minimum.

To investigate the effect of EMS on solidification, a coupled simulation of solidification and EMS model has been compared with the solidification model without EMS. It can be seen from Figure 4(a) that without EMS, the smooth solid shell has been formed near the mold wall while in Figure 4(b), a break in solid shell formation or increase in liquid fraction near the stirrer has been found after application of EMS. This

break in solid shell formation is due to the centrifugal force generated because of rotary motion of fluid which moves the overheated liquid steel from the core of mold towards the mold wall leading to increase in temperature near the mold wall. In Figure 5(a), liquid steel core can clearly be seen at the mold axial central plane when EMS has not been applied, however in Figure 5(b), a mushy zone can be seen at the center of the mold when EMS model has been used. It shows the mixing of liquid core (at high-temperature) with the low-temperature mushy region near the wall. Thus, there is forced convection

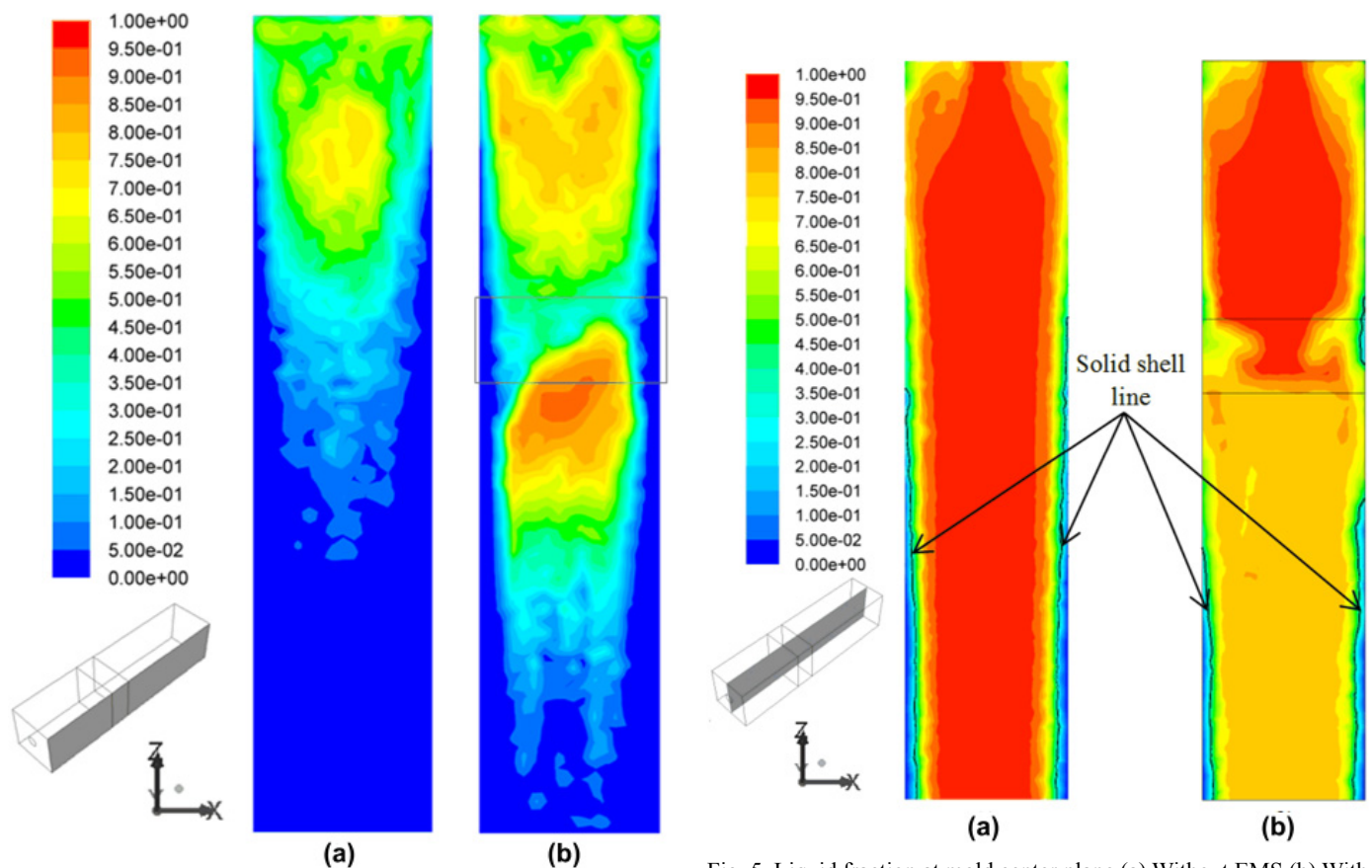


Fig. 4. Liquid fraction at mold wall (a) Without EMS (b) With EMS

Fig. 5. Liquid fraction at mold center plane (a) Without EMS (b) With EMS

flow within the mold due to EMS and finally some reduction in the temperature gradient near the solidification front. It has been stated by Kurz et al. [33] that low-temperature gradient generally promotes the formation of equiaxed grains, as grain morphologies are directly influenced by the temperature gradient. So, by the use of EMS, temperature gradient near solidification front is reduced to some extent and in turn, expected to promote the equiaxed grain formation.

#### 4.1. Effect of electromagnetic frequency

Investigation of the effect of electromagnetic frequency has been carried out by simulating the coupled solidification and EMS model at four different frequencies i.e. 2 Hz, 5 Hz, 10 Hz and 20 Hz with a magnetic flux density of 0.1 Tesla. The four frequencies were selected to study from low to high electromagnetic stirring frequencies. The results have also been compared with the results of individual solidification model and EMS model. Figure 6(a) shows fluid flow pathlines in the mold on applying solidification model without EMS and Figure 6(b) shows the pathlines of fluid flow after applying EMS model without solidification. Figure 6(c-f) shows the pathlines on applying EMS along with solidification for different frequencies. Without the use of EMS, pathlines are shown to be in a vertically downward direction (Fig. 6a) while the use of EMS is seen to

alter the pattern of these pathlines. It is seen that use of EMS induces a circular motion starting from the region where EMS is applied. On applying EMS without solidification, circular motion of fluid are found till the bottom of the mold, as shown in Figure 6(b) whereas in Figure 6(c-f), circular motion of fluid are found to gradually diminishes while moving below the stirrer position when solidification model is activated. This is due to the formation of the mushy zone formed during solidification. From Figure 6(c-f), it is also observed that axial length of stirring below the stirrer position decreases as the frequency of magnetic field increases. As axial length of stirring reduces the segregation [6] low-frequency magnetic field provides better segregation reduction as compared to that by the high-frequency magnetic field in EMS.

Figure 7(a-e) shows the liquid fraction contours at the mold exit for different cases with and without applying electromagnetic stirring. The presence of liquid core at the center of the mold can be seen in Figure 7(a) when EMS has not been applied. After applying EMS with varying frequencies, the mushy zone is found to replace the liquid core at the mold center, as shown in Figure 7(b-e). Mushy zone at the mold center is formed because of forced convection in  $x$ - $y$  direction caused by the circular motion of the fluid. It is clearly seen from Figure 7(b-e) that as the frequency of magnetic field increases, the liquid fraction of steel at the center of mold exit decreases. This can better be understood by referring to Figure 8, which graphically depicts

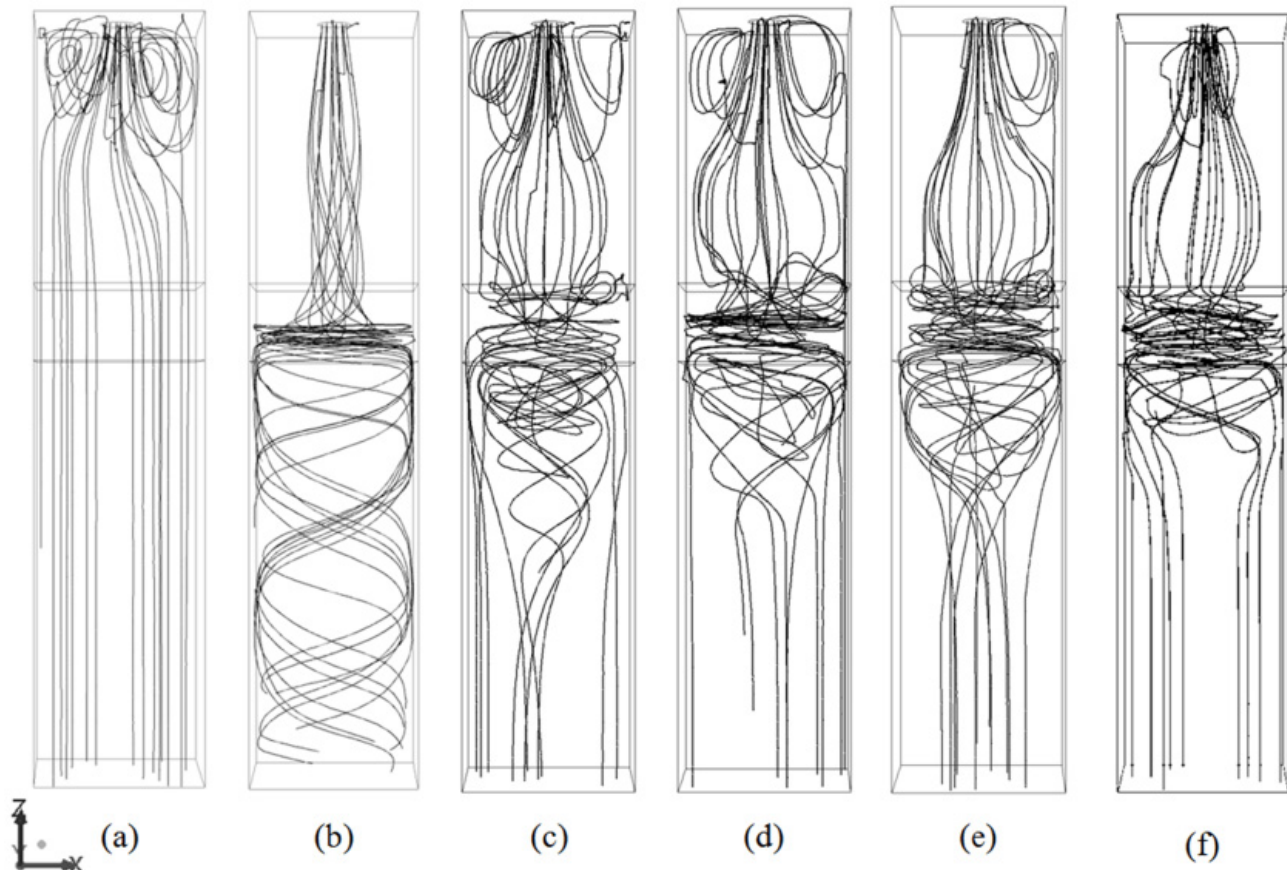


Fig. 6. Fluid flow pathlines (a) solidification without EMS (b) EMS without solidification, and solidification with EMS at frequency (c) 2 Hz (d) 5 Hz (e) 10 Hz (f) 20 Hz

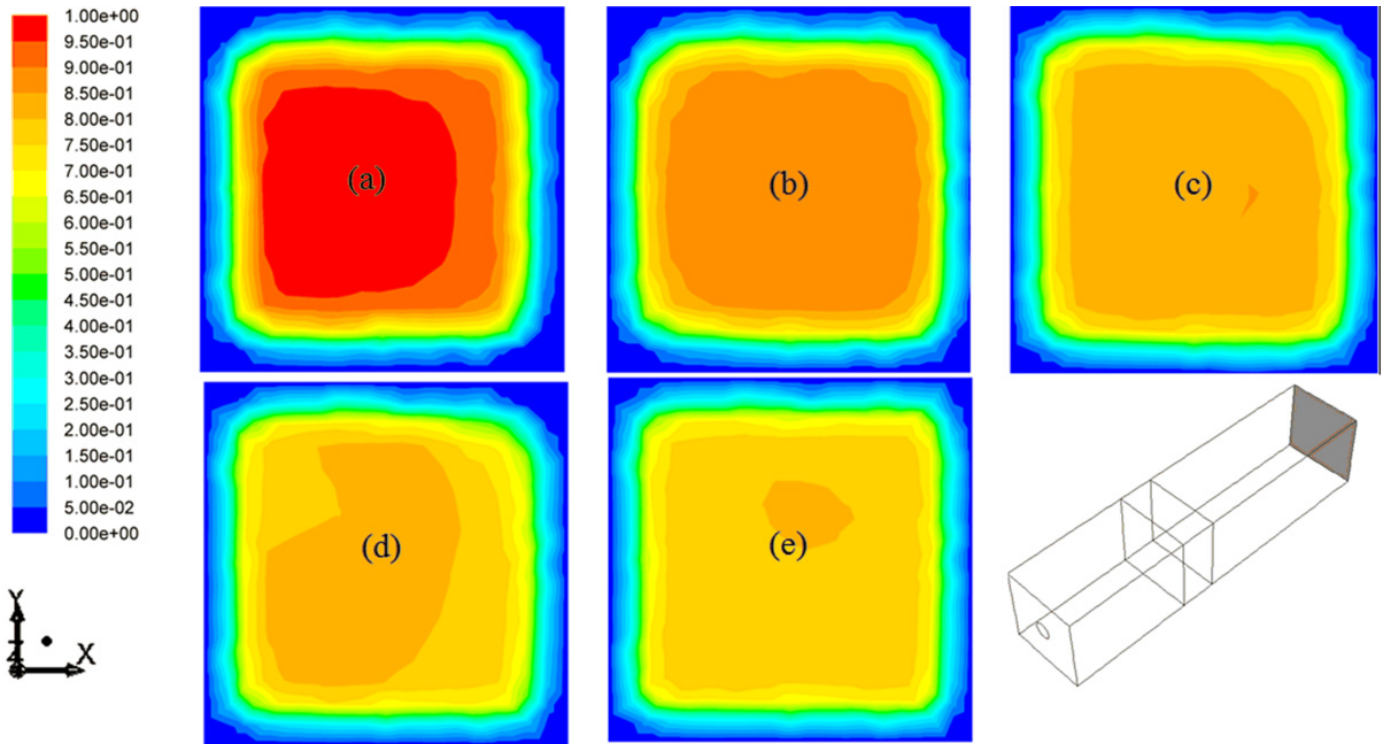


Fig. 7. Liquid fraction at mold outlet (a) without EMS, and with EMS at frequencies (b) 2 Hz (c) 5 Hz (d) 10 Hz (e) 20 Hz

the liquid fraction at the mold outlet for with and without EMS. It is seen that without EMS, the liquid fraction values in the core region i.e. the central portion of the  $x$ -axis domain is nearly 1 indicating the temperature just below liquidus. As electromagnetic stirring is applied with a frequency of 2 Hz, the temperature of the central region falls because of mixing of the central region liquid with solidified region near the mold wall. This results in a decrease in liquid fraction value in the central region and a small increase in temperature towards the region away from the central core. In fact, the increase in the horizontal length of the curve once electromagnetic stirring is applied indicates the increase in uniformity in liquid fraction or temperature at the central portion of the mold. As the frequency of the magnetic

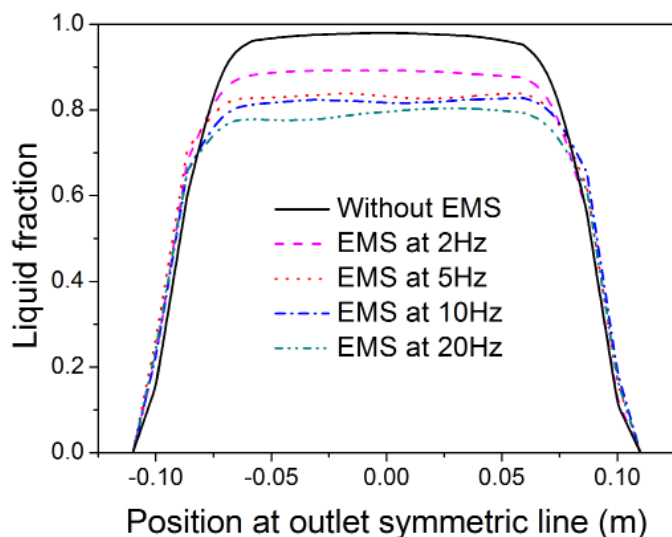


Fig. 8. Liquid fraction at mold outlet symmetric line

field is increased, the stirring effect is seen to make the temperature more and more uniform leading to a gradual decrease in the liquid fraction values at the center of mold exit. An increase in liquid fraction, though a very small amount, near the mold wall decreases the thermal gradient in that region and prevents the growth of grains towards the central core region. In other words, an equiaxed type of grains is more favorably formed in place of columnar grains. With the increase in magnetic field frequency, it is observed that as the thermal gradient decreases, chances of equiaxed grain formation increases.

Previously reported literature have mentioned that mushy zone having liquid fraction 0.0-0.5 behaves like solid [34] and above this further change in grain structure due to solidification is least possible. In the present study, for finding the solid shell thickness near the mold wall, it is assumed that steel having a liquid fraction of 0.3 is completely solidified. In Figure 9 (a-e), an iso-surface of liquid fraction 0.3 has been plotted on the vertical plane i.e.  $X$ - $Z$  plane at the center of the mold. From Figure 9(a), it is seen that in the absence of EMS, solidified shell formation starts at a distance of  $\sim 300$  mm down the meniscus. On applying EMS at 2 Hz magnetic frequency, nearly similar solid shell thickness below meniscus can be observed in Figure 9(b), as with the case without EMS. Except the fact that the solid shell thickness in the stirred region is somewhat less though the shell thickness at the exit of the mold seems to be same. On increasing the stirrer magnetic frequency above 2 Hz, a change in the solid shell is found below the EMS position, as shown in Figure 9(c-e). It is observed facts that increase in magnetic field frequency confines the Lorentz force near the stirrer boundary layer and has more penetration in the solid shell. Hence, decrease or break in the solid shell is found on increasing the field frequency. In

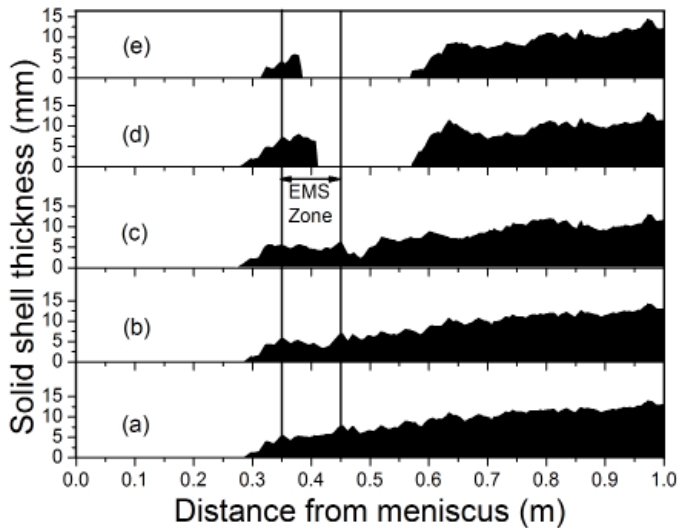


Fig. 9. Solid shell thickness at the center of mold wall, below the meniscus for cases (a) without EMS, and with EMS at frequencies (b) 2 Hz (c) 5 Hz (d) 10 Hz (e) 20 Hz

Figure 9(c), at 5 Hz frequency, a decrease in the solidified shell is observed near 480 mm down the meniscus. This is because of the dissolution of the solidified shell by mixing of the liquid core of the central portion of the mold with the solidified shell at the side, due to which the solidified shell remelts and transforms to liquid and gets uniformly mixed. As the magnetic frequency increases further to 10 Hz, the re-melting or the dissolution of the solidified shell occurs early, i.e. at a distance of 410 mm down the meniscus and onset of solidified shell formation for the second time is seen to occur at a distance of 570 mm down the meniscus. As the frequency is further increased to 20 Hz, the trend remains nearly the same except there is a break in solidified shell. This means that as the frequency is increased, the solidified shell remelts early and more strongly. This may be due to the increase in circular or tangential velocity of the fluid by increasing the frequency, which results in an increase in the magnitude of forced convection effects in molten steel. The change in magnitude of tangential velocity can be seen by referring to Figure 10 in which the tangential velocity is plotted on a lateral axis 450 mm below the meniscus level i.e. just below the position where stirrer is placed. It is seen that near the solidification front, the fluid has high tangential velocity and decreases gradually to zero at the central axis of mold. Increase in tangential velocity near solidification front with the increase in magnetic frequency is also observed. High tangential velocity near the solidification front breaks the coarse dendritic grains into fine grains. Maximum tangential velocity near the solidification front is found for EMS at 20 Hz magnetic frequency, hence expected to give more fine grain structure. However, as the temperature gradient after the gap (onset of the second solidified shell formation) is likely to increase, an unfavorable condition for equiaxed grains formation during solidification in continuous casting process arises.

From Figure 9 (a-e), it is also observed that solid shell thickness at the mold exit is nearly equal for all the cases. It so

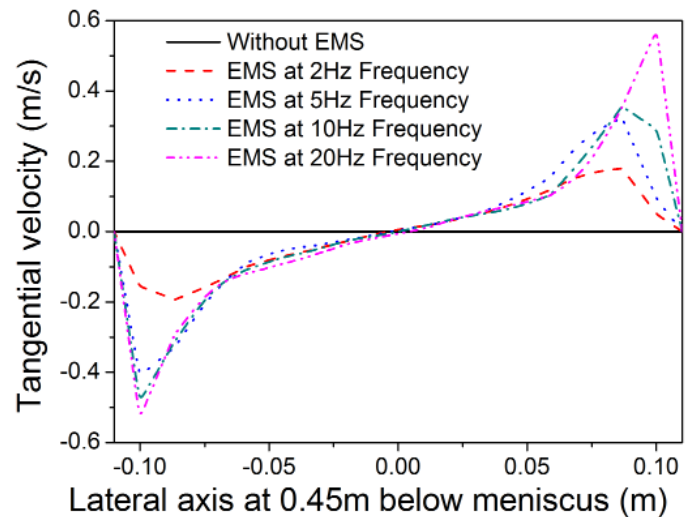


Fig. 10. Tangential velocity for different frequencies

happens that as the liquid metal from the central portion comes on the near the mold wall, the heat removal rate is increased from the mold surface because of increase in mold surface temperature. So the rate of formation of solidified shell increases and immediately a thick solidified shell is formed in the cases when EMS is applied. It would be more clear from Figure 11, where the average mold wall heat flux for the case without EMS is found to decrease gradually down the mold while, after applying EMS, the wall heat flux below the stirrer position increases relatively with the case without EMS. On applying EMS the maximum increase in wall heat flux from the case without EMS is found for the EMS with 20 Hz frequency as it also has a maximum gap in the solidified shell. This increase in wall heat flux is due to increase in mold surface temperature in the stirred region. The increase in wall heat flux quickly decreases the surface temperature of the mold and becomes equivalent to the without EMS case. Hence, the final shell thickness does not increase much in all the cases.

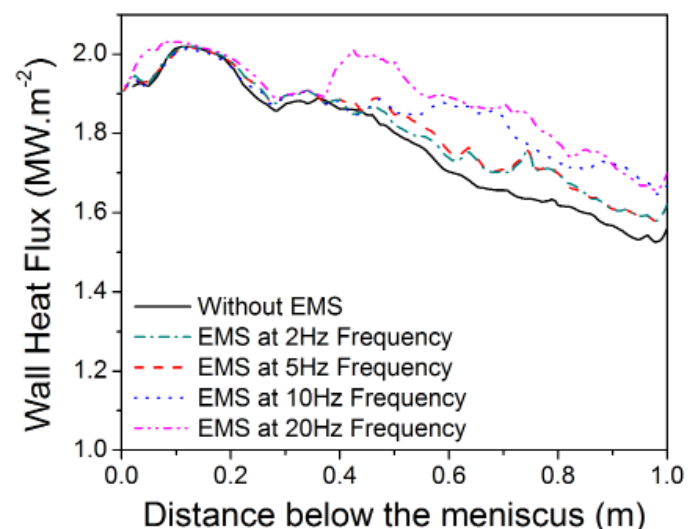


Fig. 11. Average wall heat flux for different frequencies

#### 4.2. Effect of magnetic flux density

Magnetic flux density plays a vital role in the application of EMS in continuous casting of steel though it has limitations too. Hence, the optimum flux density should be applied during electromagnetic stirring in continuous casting. Four different magnetic flux densities have been applied to analyze its effect on solidification in billet caster mold. The frequency of the magnetic field has been kept constant to 10 Hz as it is a moderate frequency in the range where significant changes have been observed in the previous section. Figure 12(a-d) shows the fluid flow pathlines in the mold at four different magnetic flux density values of 0.05, 0.1, 0.15 and 0.2 Tesla respectively. It is clearly observed that with the increase in magnetic flux density, the intensity of stirring of fluid increases in the zone of the stirrer and to some extent in the downward vicinity of the stirrer. In Figure 12(a), when the intensity of stirring is very low at 0.05 T, there seems to be an insufficient electromagnetic force to stir the liquid steel because the stirring effect is not seen reach near the wall of the mold. As the flux density is increased, the vigorous rotation causes the fluid from the center to be in intimate contact with the side walls of the mold and further it rotates to touch the wall on the other side of the mold. This process continues inside the stirrer zone and ensures complete mixing of central core region full of fluid with thin solidified skin on the mold walls.

Figure 13(a-e) shows the contours of the liquid fraction at mold exit for without magnetic field and with different magnetic flux densities. In the line of predicted fluid flow pathlines shown in Figure 12 where EMS at 0.05 T of magnetic field shows very less stirring intensity effect, can be seen in Figure 13(b) that

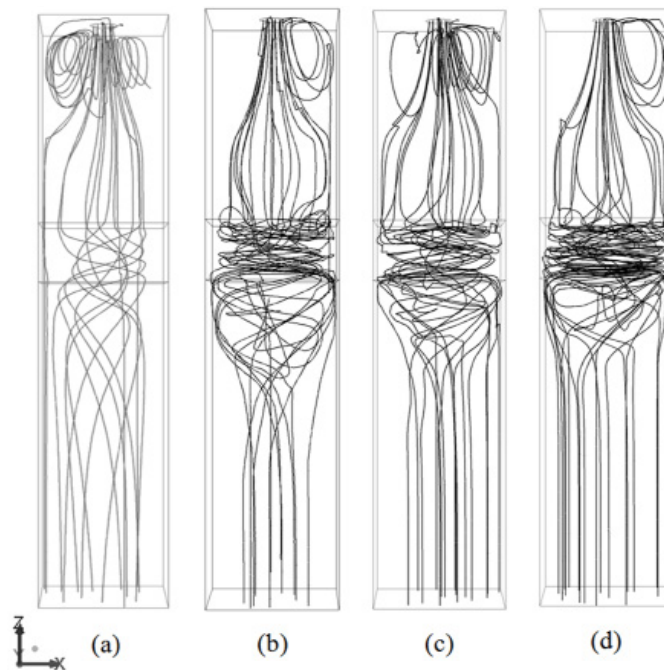


Fig. 12. Fluid flow pathlines during solidification with EMS at magnetic flux density (a) 0.05 T (b) 0.10 T (c) 0.15 T (d) 0.20 T

liquid core still exists after the application of magnetic field because of very low flux density. Because of insufficient stirring effect, a small portion is still in liquid state, similar to that observed for without EMS case. However, a decrease in liquid fraction or mushy zone can be seen at the center of mold exit, as shown in Figure 13(c-e) when the magnetic flux density is increased. The value of liquid fraction seems to be decreasing

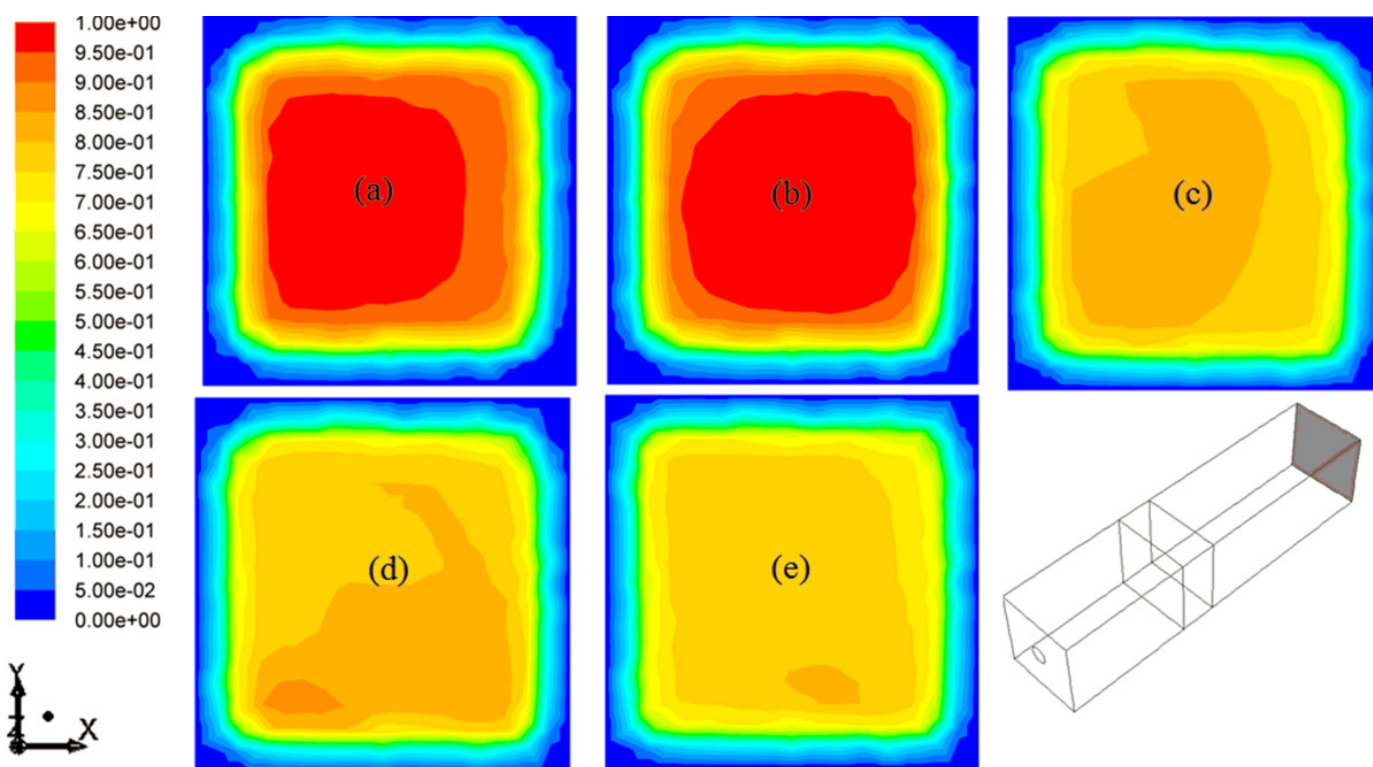


Fig. 13. Liquid fraction at mold outlet (a) Without EMS, and with EMS at magnetic flux density (b) 0.05 T (c) 0.10 T (d) 0.15 T (e) 0.20 T

continuously with increase in magnetic flux density. The liquid fraction of steel for different magnetic flux densities at the mold outlet symmetric line along the  $x$ -axis is shown graphically in Figure 14. It can be observed that there is not much change in the graphs of the liquid fraction of without EMS and with EMS at 0.05 T magnetic flux density. Maximum change in liquid fraction was observed as 0.3 for the EMS with 0.20 T, which is very close to liquid fraction obtained from EMS at 0.1 T and 0.15 T magnetic flux density. The increase in magnetic flux density of the stirrer decreases maximum liquid fraction and so the temperature gradient of steel near the solid front. As the change in liquid fraction above 0.1 T is low, it is suggested not to use high magnetic flux density.

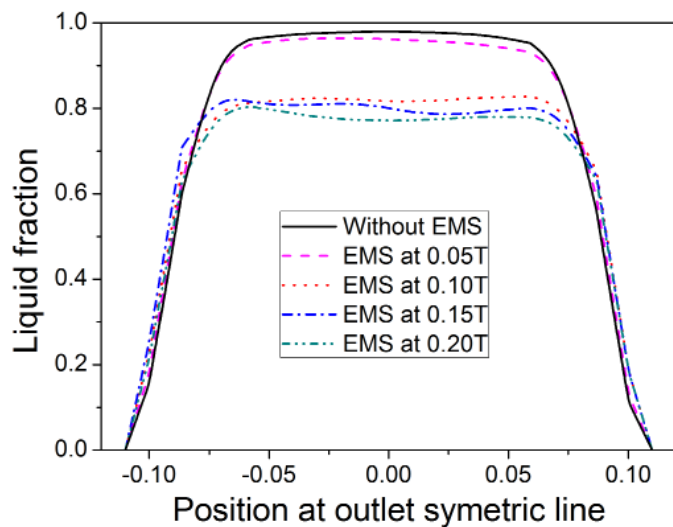


Fig. 14. Liquid fraction at mold outlet symmetric line

At different magnetic flux density of EMS, thickness of solid shell formed at the center of mold wall while moving below the meniscus is shown in Figure 15(a-e). Growth in solid shell thickness for 0.05 T has been found to be similar as with the without EMS case. A break in solid shell below the EMS position has been observed when magnetic flux density is increased above 0.10 T, as shown in Figure 15(c-e). It can be noticed that the width of gap increases with the increase in magnetic flux density. Formation of these gaps and increase in width with the increase in magnetic flux density are due to increase in stirring intensity and increase in tangential velocity of the fluid. Figure 16 shows tangential velocities for different magnetic flux densities on a lateral axis at 0.45 m below the meniscus. It can be observed that tangential velocity near the solidification front increases with the increase in magnetic flux density. The increase in tangential velocity increases forced convection in steel and hence increases the temperature near solidification front due to which gap in the solid shell is formed, as discussed in the previous section. It can also be predicted that high magnetic field EMS is a favorable condition towards the fine dendritic grain structure formation in a new solid shell formed after the re-melting due to stirring, as it has high tangential velocity near the solidification front.

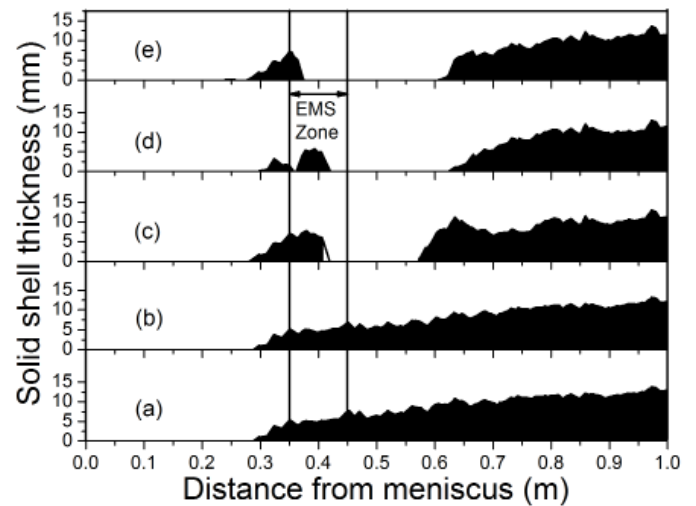


Fig. 15. Solid shell formation at the mold wall, below the meniscus for cases (a) Without EMS, and with EMS at magnetic flux density (b) 0.05T (c) 0.10T (d) 0.15T (e) 0.20T

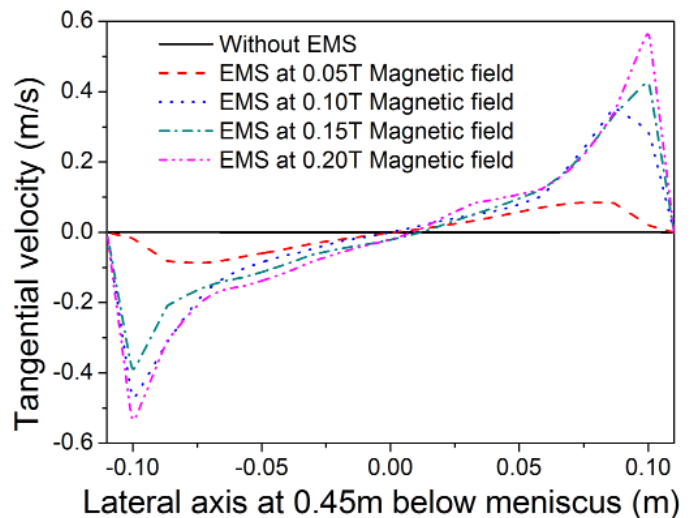


Fig. 16. Tangential velocity for different magnetic flux densities

## 5. Conclusions

A 3-dimensional model of a billet caster mold has been prepared to analyze the effect of electromagnetic stirring on the solidification of steel within the mold. It involves the simultaneous solution of fluid flow, solidification, and electromagnetic equations. From the results, the following conclusions can be made.

The rotary motion of fluid made by EMS imparts high velocity at the periphery and decreases gradually towards the center. This high rotational flow near the solidification front could break the coarse dendritic structure and may transform it to a finer grain. Tangential velocity of the liquid steel increases with the increase of magnetic frequency and magnetic flux density.

The liquid fraction at the center of mold and temperature gradient near the solidification front decreases with increase in magnetic flux density. Thus, high magnetic flux density may promote to form equiaxed grain structure.

From the pathlines of fluid flow, it may be inferred that the length of stirring decreases with the increase in magnetic frequency while, the intensity of stirring in the stirrer region increases with the increase in magnetic flux density. As the length of stirring reduces centerline segregation, low-frequency EMS is preferred to reduce centerline segregation.

From the results obtained, the optimum characteristics of the stirrer is preferred to have low or medium magnetic frequency and high flux density for taking their combined effect on the fluid flow and solidification in the mold.

#### REFERENCES

- [1] M. Javurek, M. Barna, P. Gittler, K. Rockenschaub, M. Lechner, *Steel Res. Int.* **79**, 617-626 (2008).
- [2] T. Toh, H. Hasegawa, H. Harada, *ISIJ Int.* **41**, 1245-1251 (2001).
- [3] T.T. Natarajan, N. El-Kaddah, *Appl. Math. Model.* **28**, 47-61 (2004).
- [4] M. Rywotycki, Z. Malinowski, J. Gielżecki, A. Gołdasz, *Arch. Metall. Mater.* **59**, 487-492 (2014).
- [5] H. Nakata, T. Inoue, H. Mori, K. Ayata, T. Murakami, T. Komina, *ISIJ Int.* **42**, 264-272 (2002).
- [6] X.P. Song, S.S. Cheng, Z.J. Cheng, *Ironmak. Steelmak.* **40**, 189-198 (2013).
- [7] K. Stransky, F. Kavicka, B. Sekanina, J. Stetina, V. Gontarev, J. Dobrovska, *Mater. Technol.* **45**, 163-166 (2011).
- [8] T. Toh, E. Takeuchi, M. Hojo, H. Kawai, S. Matsumura, *ISIJ Int.* **37**, 1112-1119 (1997).
- [9] P.P. Sahoo, A. Kumar, J. Halder, M. Raj, *ISIJ Int.* **49**, 521-528 (2009).
- [10] N. Govindaraju, B.Q. Li, *Energy Conserv. Manag.* **43**, (2002) 335-344.
- [11] B. Wang, Z.G. Yang, X.F. Zhang, Y.T. Wang, C.P. Nie, Q. Liu, et al., *Metalurgija* **54**, 327-330 (2015).
- [12] S. Wang, G.A. De Toledo, K. Välimaa, S. Louhenkilpi, *ISIJ Int.* **54**, 2273-2282 (2014).
- [13] X. Geng, X. Li, F.B. Liu, H.B. Li, Z.H. Jiang, *Ironmak. Steelmak.* **00**, 1-8 (2015).
- [14] H. Liu, M. Xu, S. Qiu, H. Zhang, *Metall. Mater. Trans. B.* **43**, 1657-1675 (2012).
- [15] B. Ren, D. Chen, H. Wang, M. Long, *Steel Res. Int.* **86**, 1104-1115 (2015).
- [16] N. El-Kaddah, T.T. Natarajan, in: *CFD in the Minerals and Process Industries (CSIRO)*, Melbourne, Australia, 339 (1999).
- [17] M. Barna, M. Javurek, J. Reiter, M. Lechner, *BHM.* **154**, 518-522 (2009).
- [18] D.J. Im, J.S. Hong, I.S. Kang, *Comput. Fluids.* **70**, 13-20 (2012).
- [19] A. Buchholz, G. Rombach, G.-U. Gruen, *Electromagnetic stirring in melting furnaces – A critical evaluation*, in: *John Grandfield (Ed.) Light Metals 2014*, John Wiley & Sons, (2014).
- [20] ANSYS®, Academic Research, Release 14.0, Help Syst. Fluent, ANSYS, Inc. (2013).
- [21] A. Maurya, P.K. Jha, *J. Inst. Eng. Ser. C.* **48**, 45-52 (2017).
- [22] D. Jiang, M. Zhu, *Steel Res. Int.* **85**, 1-11 (2014).
- [23] M.R.R.I. Shamsi, S.K. Ajmani, *ISIJ Int.* **47**, 433-442 (2007).
- [24] M. Bielnicki, J. Jowsa, A. Cwudziński, *Arch. Metall. Mater.* **60**, 257-262 (2015).
- [25] T.H. Shih, W.W. Liou, A. Shabbir, Z. Yang, J. Zhu, *Comput. Fluids.* **24**, 227-238 (1995).
- [26] P.K. Jha, S.K. Dash, S. Kumar, *ISIJ Int.* **41**, 1437-1446 (2001).
- [27] P.K. Jha, S.K. Dash, *Int. J. Numer. Methods Heat Fluid Flow.* **14**, 953-979 (2004).
- [28] M. Rywotycki, K. Miłkowska-Piszczyk, L. Trębacz, *Arch. Metall. Mater.* **57**, 386-393 (2012).
- [29] Z. Malinowski, T. Telejko, B. Hadała, *Arch. Metall. Mater.* **57**, 325-351 (2012).
- [30] M. Fabbri, F. Galante, F. Negrini, E. Takeuchi, T. Toh, *COMPEL Int. J. Comput. Math. Electr. Electron. Eng.* **22**, 10-19 (2003).
- [31] A. Jonayat, B.G. Thomas, *Metall. Mater. Trans. B.* **45**, 1842-1864 (2014).
- [32] H. Nakato, M. Ozawa, K. Kinoshita, Y. Habu, T. Emi, *Trans. ISIJ.* **24**, 957-965 (1984).
- [33] W. Kurz, C. Bezencon, M. Gaumann, *Sci. Technol. Adv. Mater.* **2**, 185-191 (2001).
- [34] M. M'Hamdi, G. Lesoult, E. Perrin, J.M. Jolivet, *ISIJ Int.* **36**, S197-S200 (1996).